



In vitro metabolic fate of nine LSD-based new psychoactive substances and their analytical detectability in different urinary screening procedures

Lea Wagmann¹ · Lilian H. J. Richter¹ · Tobias Kehl¹ · Franziska Wack¹ · Madeleine Pettersson Bergstrand^{1,2,3} · Simon D. Brandt⁴ · Alexander Stratford⁵ · Hans H. Maurer¹ · Markus R. Meyer¹

Received: 12 November 2018 / Revised: 11 December 2018 / Accepted: 17 December 2018 / Published online: 7 January 2019

© Springer-Verlag GmbH Germany, part of Springer Nature 2019

Abstract

The market of new psychoactive substances (NPS) is characterized by a high turnover and thus provides several challenges for analytical toxicology. The analysis of urine samples often requires detailed knowledge about metabolism given that parent compounds either may be present only in small amounts or may not even be excreted. Hence, knowledge of the metabolism of NPS is a prerequisite for the development of reliable analytical methods. The main aim of this work was to elucidate for the first time the pooled human liver S9 fraction metabolism of the nine *d*-lysergic acid diethylamide (LSD) derivatives 1-acetyl-LSD (ALD-52), 1-propionyl-LSD (1P-LSD), 1-butyryl-LSD (1B-LSD), *N*⁶-ethyl-nor-LSD (ETH-LAD), 1-propionyl-*N*⁶-ethyl-nor-LSD (1P-ETH-LAD), *N*⁶-allyl-nor-LSD (AL-LAD), *N*-ethyl-*N*-cyclopropyl lysergamide (ECPLA), (2'*S*,4'*S*)-lysergic acid 2,4-dimethylazetidide (LSZ), and lysergic acid morpholide (LSM-775) by means of liquid chromatography coupled to high-resolution tandem mass spectrometry. Identification of the monooxygenase enzymes involved in the initial metabolic steps was performed using recombinant human enzymes and their contribution confirmed by inhibition experiments. Overall, *N*-dealkylation and hydroxylation, as well as combinations of these steps predominantly catalyzed by CYP1A2 and CYP3A4, were found. For ALD-52, 1P-LSD, and 1B-LSD, deacylation to LSD was observed. The obtained mass spectral data of all metabolites are essential for reliable analytical detection particularly in urinalysis and for differentiation of the LSD-like compounds as biotransformations also led to structurally identical metabolites. However, in urine of rats after the administration of expected recreational doses and using standard urine screening approaches, parent drugs or metabolites could not be detected.

Keywords Lysergamides · NPS · Metabolism · Urinalysis · LC-HRMS/MS

Published in the topical collection *Young Investigators in (Bio-)Analytical Chemistry* with guest editors Erin Baker, Kerstin Leopold, Francesco Ricci, and Wei Wang.

Electronic supplementary material The online version of this article (<https://doi.org/10.1007/s00216-018-1558-9>) contains supplementary material, which is available to authorized users.

✉ Markus R. Meyer
markus.meyer@uks.eu

¹ Department of Experimental and Clinical Toxicology, Institute of Experimental and Clinical Pharmacology and Toxicology, Center for Molecular Signaling (PZMS), Saarland University, Kirrberger Str. 100, 66421 Homburg, Germany

² Department of Laboratory Medicine, Division of Clinical Pharmacology, Karolinska Institutet, Stockholm, Sweden

³ Department of Laboratory Medicine, Division of Clinical Chemistry, Karolinska Institutet, 17177 Stockholm, Sweden

⁴ School of Pharmacy and Biomolecular Sciences, Liverpool John Moores University, Byron Street, Liverpool L33AF, UK

⁵ Synex Synthetics BV, Karveelweg 20, 6222NH Maastricht, The Netherlands

Introduction

The discovery of the potent psychoactive effects of *d*-lysergic acid diethylamide (LSD, see Fig. 1) in 1943 triggered a new era in psychopharmacological research and subsequently became a household name in popular culture [1]. For the purpose of extending the knowledge of lysergamide-based structure-activity relationships, several LSD-based substances have been investigated [2–9]. In recent years, a renewed interest in the use of LSD within the clinical context emerged as documented by increasing numbers of studies involving human volunteers [10–12]. At the same time, a number of LSD-based substances appeared as “research chemicals” on the new psychoactive substances (NPS) market, predominantly in the form of blotters and powders. These substances included 1-acetyl-LSD (ALD-52), 1-propionyl-LSD (1P-LSD) [13], 1-butyryl-LSD (1B-LSD), *N*⁶-ethyl-nor-LSD (ETH-LAD) [14], 1-propionyl-ETH-LAD (1P-ETH-LAD) [14], *N*⁶-allyl-nor-LSD (AL-LAD) [15], *N*-ethyl-*N*-cyclopropyl lysergamide (ECPLA) [16], (2′*S*,4′*S*)-lysergic acid 2,4-dimethylazetidide (LSZ) [15], and lysergic acid morpholide (LSM-775) [17] (Fig. 1).

NPS in general were reported to the EU Early Warning System at a rate of one per week in 2016 being a big issue in forensic or clinical toxicology and the health care system in general [18]. The ability to detect newly emerging drugs of abuse in samples obtained from biological matrices requires the development of reliable screening methods. In particular, the analysis of urine samples benefits from knowing the drug’s metabolic transformation patterns, especially in cases where

the parent compound may only be present in small amounts or not even be excreted. In the case of LSD, its metabolite 2-oxo-3-hydroxy LSD was reported to be present at higher concentrations and detectable for a longer time than LSD itself in urine samples of LSD users [19]. The detection of 2-oxo-3-hydroxy LSD in urine has been subsequently described as part of some clinical investigations [20, 21]. In vivo studies in rodents or in vitro studies using human hepatocytes or human liver cell fractions such as pooled human liver microsomes (pHLM) or pooled human liver S9 (pS9) are established tools for metabolite formation and subsequent identification [22–25]. Several studies showed comparable metabolic profiles to human urine samples [26–28]. To date, no information on the phase I and II metabolism of the nine LSD derivatives investigated in this study is available. Therefore, the aim of the present study was first to identify the main in vitro phase I and II metabolites of ALD-52, 1P-LSD, 1B-LSD, ETH-LAD, 1P-ETH-LAD, AL-LAD, ECPLA, LSZ, and LSM-775 for toxicological screening purposes using pS9 incubations and subsequent analysis by liquid chromatography coupled to high-resolution tandem mass spectrometry (LC-HRMS/MS). LSD was also investigated and results compared to literature to aid development of the experimental conditions. In addition, the monooxygenase enzymes involved in the initial metabolic steps were investigated to assess the potential impact of inter-individual variations that may occur during metabolism or as a consequence of drug–drug and drug–food interactions. As no information about the monooxygenases involved in the metabolism of LSD is available so far, it was also included in this study. Finally, detectability studies using rat urine collected

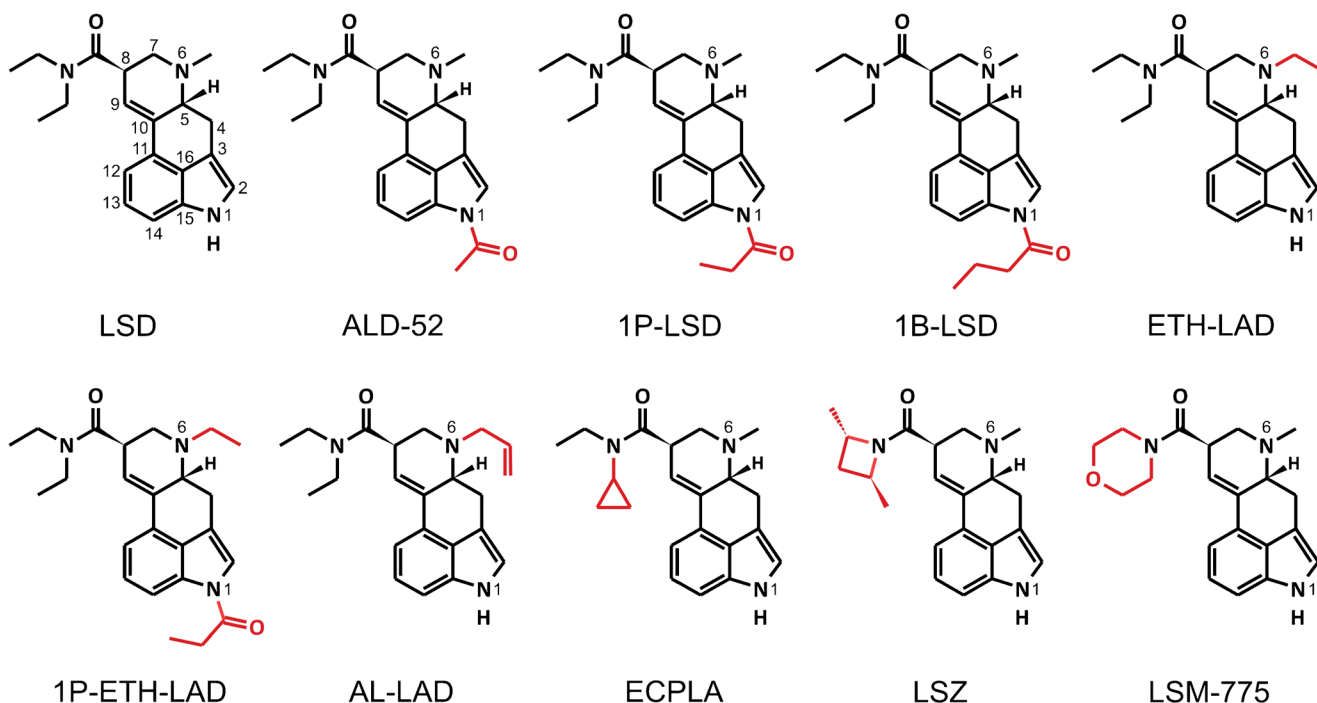


Fig. 1 Chemical structures of LSD and nine LSD-based new psychoactive substances. Structural changes in comparison to LSD are marked in red

after the administration of expected recreational doses of the LSD-based NPS and standard urine screening approaches (SUSAs) were conducted.

Experimental

Chemicals and enzymes

ALD-52, 1P-LSD, 1B-LSD, ETH-LAD, 1P-ETH-LAD, AL-LAD, ECPLA, LSZ, and LSM-775 were available from previous studies and provided by Synex Synthetics (Maastricht, The Netherlands). LSD and LSD- d_3 were supplied by LGC Standards (Wesel, Germany). Isocitrate, isocitrate dehydrogenase, superoxide dismutase, 3'-phosphoadenosine-5'-phosphosulfate (PAPS), *S*-(5'-adenosyl)-*L*-methionine (SAM), dithiothreitol (DTT), reduced glutathione (GSH), carnitine acetyltransferase, acetylcarnitine, acetyl coenzyme A (AcCoA), magnesium chloride ($MgCl_2$), potassium dihydrogenphosphate (KH_2PO_4), dipotassium hydrogenphosphate (K_2HPO_4), Tris hydrochloride, ketoconazole, and alpha-naphthoflavone from Sigma-Aldrich (Taufkirchen, Germany), and $NADP^+$ were from Biomol (Hamburg, Germany). Acetonitrile (LC-MS grade), ammonium formate (analytical grade), formic acid (LC-MS grade), methanol (LC-MS grade), and all other chemicals and reagents (analytical grade) were from VWR (Darmstadt, Germany). The baculovirus-infected insect cell microsomes (Supersomes) containing 1 nmol/mL of human cDNA-expressed CYP1A2, CYP2A6, CYP2B6, CYP2C8, CYP2C9 (2 nmol/mL), CYP2C19, CYP2D6, CYP2E1 (2 nmol/mL), CYP3A4, CYP3A5 (2 nmol/mL), or FMO3 (5 mg protein/mL), and pHLM (20 mg microsomal protein/mL, 330 pmol total CYP/mg protein), pS9 (20 mg microsomal protein/mL), UGT reaction mixture solution A (25 mM UDP-glucuronic acid), and UGT reaction mixture solution B (250 mM Tris HCl, 40 mM $MgCl_2$, and 125 μ g/mL alamethicin) were obtained from Corning (Amsterdam, The Netherlands). After delivery, the enzymes and liver cell preparations were thawed at 37 °C, aliquoted, snap-frozen in liquid nitrogen, and stored at -80 °C until use. LSD and all other lysergamide test drugs were dissolved in methanol at a concentration of 1 mg/mL, each, and stored at -20 °C.

In vitro incubations for metabolism studies

As previously described by Richter et al. [29], the final incubation volume was 150 μ L. Incubations were performed using pS9 (2 mg microsomal protein/mL) after preincubation for 10 min at 37 °C with 25 μ g/mL alamethicin (UGT reaction mixture solution B), 90 mM phosphate buffer (pH 7.4), 2.5 mM Mg^{2+} , 2.5 mM isocitrate, 0.6 mM $NADP^+$, 0.8 U/mL isocitrate dehydrogenase, 100 U/mL superoxide

dismutase, 0.1 mM AcCoA, 2.3 mM acetylcarnitine, and 8 U/mL carnitine acetyltransferase. Thereafter, 2.5 mM UDP-glucuronic acid (UGT reaction mixture solution A), 40 μ M PAPS, 1.2 mM SAM, 1 mM DTT, 10 mM GSH, and 25 μ M substrate (LSD or analog) were added. All given concentrations are the final concentrations in one reaction tube. The organic solvent content in the final incubation mixtures was always below 1% [30]. The reaction was initiated by addition of substrate and the reaction mixture was incubated for a maximum of 480 min. After 60 min, an aliquot of 60 μ L of the incubation mixture was transferred to a reaction tube containing 20 μ L ice-cold acetonitrile for termination of the reactions. The remaining mixture was incubated for additional 420 min and thereafter stopped by addition of 30 μ L ice-cold acetonitrile. Afterwards, mixtures were cooled for 30 min at -18 °C, centrifuged for 2 min at 18,407 \times g (rcf), and a volume of 60 μ L of the supernatants transferred into autosampler vials, followed by injection of 1 μ L onto the LC-HRMS/MS system. Blank samples without substrate and control samples without pS9 were prepared to confirm the absence of interfering compounds and to identify compounds not formed by metabolism, respectively. All incubations were performed in duplicates ($n = 2$).

Monoxygenases activity screening and inhibition studies using selective CYP inhibitors

According to previously published procedures [31], microsomal incubations ($n = 2$ each) were performed at 37 °C for 30 min using a substrate concentration of 25 μ M (LSD or analog) and CYP1A2, CYP2A6, CYP2B6, CYP2C8, CYP2C9, CYP2C19, CYP2D6, CYP2E1, CYP3A4, CYP3A5 (75 pmol/mL each), or FMO3 (0.25 mg protein/mL). Reference incubations with pHLM (1 mg microsomal protein/mL) were used as positive control. Control samples without enzymes were prepared to assess formation of compounds that did not originate from metabolism. Besides enzymes and substrates, the incubation mixtures (final volume, 50 μ L) contained 90 mM phosphate buffer (pH 7.4), 5 mM Mg^{2+} , 5 mM isocitrate, 1.2 mM $NADP^+$, 0.5 U/mL isocitrate dehydrogenase, and 200 U/mL superoxide dismutase. For incubations with CYP2A6 or CYP2C9, phosphate buffer was replaced with 90 mM Tris buffer, respectively, according to the manufacturer's recommendation. Reactions were initiated by addition of the enzyme preparation and terminated by addition of 50 μ L of ice-cold acetonitrile, containing 5 μ M LSD- d_3 as internal standard. The mixture was centrifuged for 2 min at 18,407 \times g (rcf). Seventy microliters of the supernatant was transferred into an autosampler vial and 1 μ L was injected into the LC-HRMS/MS system.

According to a previous study [32], the influence of ketoconazole (CYP3A4 inhibitor), alpha-naphthoflavone (CYP1A2 inhibitor), or a mixture of them (1 μ M,

respectively) on the formation of monooxygenase-dependent metabolites was assessed using pHLM (1 mg microsomal protein/mL), 25 μ M substrate (LSD or one of the analogs), and LSD- d_3 as internal standard. All incubations were performed at 37 °C for 20 min with six replicates in each test set. All other incubation settings were the same as described for the monooxygenases activity screening. As measure of the metabolite formation in reference incubations without inhibitors, peak areas of all metabolites were summed up and divided by the peak area of the internal standard. This was also done for control incubations without pHLM and peak area ratios were subtracted from that in reference incubations. The result was referred to as 100% and compared to peak area ratios in test incubations with inhibitors. Significance of inhibition was tested using a one-way ANOVA followed by Dunnett's multiple comparison test (significance level, $P < 0.001$, 99.9% confidence intervals) by GraphPad Prism 5.00 software (GraphPad Software, San Diego, USA).

LC-HRMS/MS instrumentation

A Thermo Fisher Scientific (TF, Dreieich, Germany) Dionex UltiMate 3000 Rapid Separation (RS) UHPLC system with a quaternary UltiMate 3000 RS pump and an UltiMate 3000 RS autosampler was used, controlled by the TF Chromeleon software version 6.80, and coupled to a TF Q-Exactive Plus equipped with a heated electrospray ionization II source (HESI-II). Mass calibration was performed prior to analysis according to the manufacturer's recommendations using external mass calibration. Gradient elution was performed on a TF Accucore PhenylHexyl column (100 mm \times 2.1 mm inner diameter, 2.6 μ m particle size). The mobile phases consisted of 2 mM aqueous ammonium formate containing formic acid (0.1%, v/v) and acetonitrile (1%, v/v, pH 3, eluent A) and 2 mM ammonium formate in acetonitrile/methanol (50:50, v/v) containing formic acid (0.1%, v/v) and water (1%, v/v, eluent B). The gradient and flow rate were programmed as follows: 0–10 min 10% B to 50% B, 10–12 min hold 98% B, and 12–14 min hold 10% B, constantly at a flow rate of 0.5 mL/min. HESI-II conditions have been employed as described previously by Wagmann et al. [33]: heater temperature, 438 °C; ion transfer capillary temperature, 269 °C; sheath gas, 53 arbitrary units (AU); auxiliary gas, 14 AU; sweep gas, 3 AU; spray voltage, 3.50 kV, and S-lens RF level, 60.0. Mass spectrometric analysis was performed in positive full-scan mode and targeted MS² mode using an inclusion list. Pick others mode was activated to ensure the recording of MS² spectra of precursor ions not in the inclusion list. The settings for full-scan data acquisition were as follows: resolution, 35,000; automatic gain control (AGC) target, 1e6; maximum injection time (IT), 120 ms; scan range, m/z 100–700. The settings for the targeted MS² mode using an inclusion list were as follows: resolution, 17,500; AGC target, 2e5; maximum IT,

250 ms; isolation window, m/z 1.0; high-collision dissociation cell with stepped normalized collision energy 17.5, 35.0, 52.5. TF Xcalibur Qual Browser software version 2.2 SP1.48 was used for data evaluation.

Collection of rat urine samples for detectability studies

In accordance with previous publications [34], the in vivo studies were performed using rat urine samples from male Wistar rats (Charles River, Sulzfeld, Germany) for toxicological diagnostic reasons according to corresponding German law (Bundesministerium der Justiz und für Verbraucherschutz, <http://www.gesetze-im-internet.de/tierschg/index.html>). Before drug administration, blank urine was collected over a period of 24 h. Animals had water ad libitum during collection of urine over a 24-h period and were housed in a metabolism cage. Urine was collected separated from feces. For the detectability studies, doses of 0.01 mg/kg body weight (BW) were administered. The urine samples were analyzed directly and remaining was aliquoted and stored at –20 °C.

Rat urine analysis by LC-HRMS/MS, LC-linear ion trap MS, and gas chromatography-MS

To check the detectability and analytical differentiation of the LSD-based NPS after estimated recreational user's dose administrations, three SUSAs were performed. The settings were used as described in the given references for the LC-HRMS/MS [35], LC linear ion trap MS (LC-MSⁿ) [36, 37], and gas chromatography (GC)-MS [38, 39] SUSAs. Briefly, the following sample preparations were used: a simple urine precipitation with acetonitrile for the LC-based SUSAs and a liquid–liquid extraction after acidic hydrolysis followed by and acetylation for the GC-MS SUSAs. Detection limits for LSD and its derivatives by the aforementioned methods were studied using methanolic pure substance solutions at various concentrations (0.1, 1, 10, and 100 ng/mL). The lowest concentration resulting in an MS² spectrum was defined as limit of identification (LOI).

Results and discussion

Identification of metabolites

Human metabolites of LSD were already described [19, 40–43]. To confirm suitable incubation conditions and detection methods concerning the in vitro assay, LSD was also incubated with pS9 and analyzed by LC-HRMS/MS. In general, MS¹ data was screened for potential exact precursor masses (PM) of expected metabolites. Afterwards, the fragmentation pattern in the MS² spectrum was interpreted and

compared to that of the parent compound for confirmation and possible assignment of the position. This procedure was the same for LSD and its analogs.

The lysergamide test drugs and all identified phase I and II metabolites are listed in Table 1, which contains their ID, the calculated exact mass of the protonated precursor ($M + H^+$), elemental composition, determined retention time (RT), and three most abundant fragment ions (FI) in MS^2 . In total, the pS9 incubations resulted in detection of several tentative metabolites: LSD, six metabolites; ALD-52, seven metabolites; 1P-LSD, eight metabolites; 1B-LSD, seven metabolites; ETH-LAD, five metabolites; 1P-ETH-LAD, seven metabolites; AL-LAD, 11 metabolites; ECPLA, eight metabolites; LSZ, nine metabolites; and LSM-775, four metabolites.

The LSD metabolites were comparable to those described before *N*-deethyl LSD (ID 2, also referred to as lysergic acid monoethylamide, LAE) and *N*⁶-demethyl LSD (ID 3, also referred to as nor-LSD) could be unambiguously identified. Two hydroxy LSD isomers were detected, but it has to be stated that the final positions of the hydroxy groups could not be determined based on fragmentation patterns. However, hydroxy LSD isomer 2 (ID 5) and the corresponding glucuronide (ID 7) are expected to be the same as described by Steuer et al. in plasma samples [42] based on their fragmentation. Dihydroxy LSD (ID 6) is expected to be the same compound referred to as 2-oxo-3-hydroxy LSD elsewhere, which is widely known as main metabolite of LSD [19, 20, 44–46]. Only the hydroxy LSD isomer with the hydroxy group located at the diethylamide part of the molecule (also referred to as lysergic acid ethyl-hydroxy ethylamide, LEO) and trihydroxy LSD were described to be present as minor signals in human plasma or urine but not detected in the in vitro pS9 incubations. However, it should be kept in mind that quantitative determinations of the metabolites' concentrations were beyond the scope of this study. Under the investigated conditions, these two metabolites might have been formed in concentrations below detectability or the chosen incubation time was not sufficient for their formation, as multistep reactions were already described to need a longer incubation time [47]. Furthermore, LSD hydroxy isomer 1 (ID 4) was expected to be hydroxylated in position 4 or 5 due to the fragmentation pattern, which was not described before (discussed in detail below for 1-depropionyl hydroxy 1P-LSD isomer 1, ID 4). Iso-LSD, a diastereomer of LSD, which is formed during the production of LSD under basic conditions, was previously used as an additional marker for LSD consumption and shown to be metabolized in the human body. The spectra of LSD and iso-LSD differed only in the intensity of particular FI [42]. For several LSD-based NPS, a smaller signal with the same mass could be detected eluting after the parent compound. The MS^2 only showed differences in the intensity of some FI, and therefore, these signals were

expected to be generated by the iso-forms. However, due to the lack of reference material, their identity could not be confirmed.

Due to the large number of LSD-based drugs used during this study, some representative examples were chosen to illustrate the general identification procedure. Furthermore, all compounds and their metabolites showed comparable fragmentation patterns. The procedure used for the tentative identification of the metabolites based on the HRMS/MS spectra was employed according to the example described for 1P-LSD (ID 11). Brandt et al. previously published an MS^2 spectrum of 1P-LSD recorded using electrospray ionization accurate mass quadrupole time of flight tandem mass spectrometry [13]. The observed fragmentation pattern corresponded to the MS^2 spectrum of 1P-LSD using orbitrap-based tandem mass spectrometry. The MS^2 spectra of LSD (ID 1) and 1P-LSD (ID 11) can be found in Fig. 2. Briefly, the FI at m/z 337.1910 ($C_{21}H_{25}N_2O_2^+$) formed after the loss of *N*-methylmethanimine (C_2H_5N) and the FI at m/z 279.1491 ($C_{18}H_{19}N_2O^+$) formed after the loss of *N,N*-diethylformamide ($C_5H_{11}NO$) from the protonated molecule ($C_{23}H_{30}N_3O_2^+$) were characteristic for 1P-LSD and allowed for a differentiation of the MS^2 spectrum of LSD since both FI carried the additional 1-propionyl moiety (C_3H_5O). These FI correspond to the FI at m/z 281.1648 ($C_{18}H_{21}N_2O^+$) and at m/z 223.1229 ($C_{15}H_{15}N_2^+$) detected in the MS^2 spectrum of LSD (Fig. 2). The last-named FI (m/z 223.1229) represented the *N*⁶-methylated 9,10-didehydroergoline core and was the FI with the highest abundance in the MS^2 spectrum of 1P-LSD, most probably formed after elimination of the *N*¹-propionyl moiety from the FI at m/z 279.1491. Also, the FI at m/z 208.0756 ($C_{14}H_{10}NO^+$) had a high abundance and was also detectable in the MS^2 spectrum of LSD. However, it has to be mentioned that a second FI with the nominal mass of m/z 208 but the exact mass of at m/z 208.0995 ($C_{14}H_{12}N_2^+$) was detectable with a comparable abundance to 208.0756 in both spectra, which was most probably formed after loss of methyl (CH_3) from FI at m/z 223.1229. In addition, the FI at m/z 128.1069 ($C_7H_{14}NO^+$) and m/z 74.0964 ($C_4H_{12}N^+$) representing the diethylamide part were detectable in the spectra of 1P-LSD and LSD. The HRMS/MS spectra of all parent compounds and the most abundant, unique metabolites after pS9 incubation allowing the identification of the parent compound (with exception of the ETH-LAD metabolite that could also be formed after intake of 1P-ETH-LAD) can be found in the Electronic Supplementary Material (ESM) in Fig. S1.

In total, eight metabolites of 1P-LSD were identified in the pS9 incubations (see Table 1). 1-Depropionylation led to the formation of LSD (ID 1, PM at m/z 324.2070). Therefore, 1P-LSD can be considered as LSD prodrug, which was consistent with preliminary data reported by Brandt et al. who incubated 1P-LSD in human serum [13]. An additional *N*-deethylation led to formation of 1-depropionyl-*N*-deethyl 1P-LSD (ID 2, PM at m/z 296.1757). The loss of an ethylene group (-28.0313 u, C_2H_4) resulted in the FI at m/z 253.1335

Table 1 LSD, ALD-52, 1P-LSD, 1B-LSD, ETH-LAD, 1P-ETH-LAD, AL-LAD, ECPLA, LSZ, LSM-775, and their phase I and II metabolites along with their identification numbers (ID), the exact mass of the protonated molecule ($M + H^+$), elemental composition, retention time(RT), and the three most abundant fragment ions (FI A-C) in MS^2 sorted by decreasing intensity. The parent compounds are given in bold and the metabolites were sorted by increasing mass and RT

ID	Compound	Exact mass, m/z	Elemental composition	RT, min	FI A	FI B	FI C
1	LSD	324.2070	C₂₀H₂₆N₃O	5.3	223.1229	208.0995	281.1648
2	<i>N</i> -Deethyl LSD	296.1757	C ₁₈ H ₂₂ N ₃ O	3.3	223.1229	208.0756	253.1335
3	<i>N</i> ⁶ -Demethyl LSD	310.1913	C ₁₉ H ₂₄ N ₃ O	5.3	209.1073	74.0964	237.1022
4	Hydroxy LSD isomer 1	340.2019	C ₂₀ H ₂₆ N ₃ O ₂	3.4	221.1073	239.1184	322.1913
5	Hydroxy LSD isomer 2	340.2019	C ₂₀ H ₂₆ N ₃ O ₂	3.6	239.1184	297.1597	224.0706
6	Dihydroxy LSD	356.1968	C ₂₀ H ₂₆ N ₃ O ₃	2.5	237.1022	74.0964	313.1552
7	Hydroxy LSD isomer 2 glucuronide	516.2340	C ₂₆ H ₃₄ N ₃ O ₈	2.0	239.1184	340.2019	224.0706
8	ALD-52	366.2176	C₂₂H₂₈N₃O₂	6.2	265.1335	223.1229	208.0756
2	1-Deacetyl- <i>N</i> -deethyl ALD-52	296.1757	C ₁₈ H ₂₂ N ₃ O	3.3	223.1229	208.0756	253.1335
3	1-Deacetyl- <i>N</i> ⁶ -demethyl ALD-52	310.1913	C ₁₉ H ₂₄ N ₃ O	5.3	209.1073	74.0964	237.1022
1	1-Deacetyl ALD-52	324.2070	C ₂₀ H ₂₆ N ₃ O	5.3	223.1229	208.0995	281.1648
9	<i>N</i> -Deethyl ALD-52	338.1863	C ₂₀ H ₂₄ N ₃ O ₂	4.5	265.1335	223.1229	295.1441
4	1-Deacetyl-hydroxy ALD-52 isomer 1	340.2019	C ₂₀ H ₂₆ N ₃ O ₂	3.4	221.1073	239.1184	322.1913
5	1-Deacetyl-hydroxy ALD-52 isomer 2	340.2019	C ₂₀ H ₂₆ N ₃ O ₂	3.6	239.1184	297.1597	224.0706
10	<i>N</i> ⁶ -Demethyl ALD-52	352.2019	C ₂₁ H ₂₆ N ₃ O ₂	6.2	251.1178	209.1073	74.0964
11	1P-LSD	380.2332	C₂₃H₃₀N₃O₂	7.2	223.1229	279.1491	208.0756
2	1-Depropionyl- <i>N</i> -deethyl-1P-LSD	296.1757	C ₁₈ H ₂₂ N ₃ O	3.3	223.1229	208.0756	253.1335
3	1-Depropionyl- <i>N</i> ⁶ -demethyl 1P-LSD	310.1913	C ₁₉ H ₂₄ N ₃ O	5.3	209.1073	74.0964	237.1022
1	1-Depropionyl 1P-LSD	324.2070	C ₂₀ H ₂₆ N ₃ O	5.3	223.1229	208.0995	281.1648
4	1-Depropionyl-hydroxy 1P-LSD isomer 1	340.2019	C ₂₀ H ₂₆ N ₃ O ₂	3.4	221.1073	239.1184	322.1913
5	1-Depropionyl-hydroxy 1P-LSD isomer 2	340.2019	C ₂₀ H ₂₆ N ₃ O ₂	3.6	239.1184	297.1597	224.0706
12	<i>N</i> -Deethyl 1P-LSD	352.2019	C ₂₁ H ₂₆ N ₃ O ₂	5.6	223.1229	279.1491	208.0756
6	1-Depropionyl-dihydroxy 1P-LSD	356.1968	C ₂₀ H ₂₆ N ₃ O ₃	2.5	237.1022	74.0964	313.1552
13	<i>N</i> ⁶ -Demethyl 1P-LSD	366.2176	C ₂₂ H ₂₈ N ₃ O ₂	7.2	209.1073	265.1335	74.0964
14	1B-LSD	394.2489	C₂₄H₃₂N₃O₂	8.0	293.1648	223.1229	208.0756
2	1-Debutyryl- <i>N</i> -deethyl-1B-LSD	296.1757	C ₁₈ H ₂₂ N ₃ O	3.3	223.1229	208.0756	253.1335
3	1-Debutyryl- <i>N</i> ⁶ -demethyl 1B-LSD	310.1913	C ₁₉ H ₂₄ N ₃ O	5.3	209.1073	74.0964	237.1022
1	1-Debutyryl 1B-LSD	324.2070	C ₂₀ H ₂₆ N ₃ O	5.3	223.1229	208.0995	281.1648
4	1-Debutyryl-hydroxy 1B-LSD isomer 1	340.2019	C ₂₀ H ₂₆ N ₃ O ₂	3.4	221.1073	239.1184	322.1913
5	1-Debutyryl-hydroxy 1B-LSD isomer 2	340.2019	C ₂₀ H ₂₆ N ₃ O ₂	3.6	239.1184	297.1597	224.0706
6	1-Debutyryl-dihydroxy 1B-LSD	356.1968	C ₂₀ H ₂₆ N ₃ O ₃	2.5	237.1022	74.0964	313.1552
15	Hydroxy 1B-LSD	410.2438	C ₂₄ H ₃₂ N ₃ O ₃	5.7	309.1597	223.1229	208.0995
16	ETH-LAD	338.2226	C₂₁H₂₈N₃O	5.6	237.1386	208.0995	309.1835
17	<i>N</i> -Deethyl ETH-LAD	310.1913	C ₁₉ H ₂₄ N ₃ O	3.6	237.1386	208.0995	281.1522
3	<i>N</i> ⁶ -Deethyl ETH-LAD	310.1913	C ₁₉ H ₂₄ N ₃ O	5.3	209.1073	74.0964	237.1022
18	Hydroxy ETH-LAD	354.2176	C ₂₁ H ₂₈ N ₃ O ₂	3.8	253.1335	297.1603	196.0762
19	Dihydroxy ETH-LAD	370.2125	C ₂₁ H ₂₈ N ₃ O ₃	2.8	251.1178	279.1128	313.1552
20	Hydroxy ETH-LAD glucuronide	530.2496	C ₂₇ H ₃₆ N ₃ O ₈	2.4	253.1335	354.2176	325.1784
21	1P-ETH-LAD	394.2489	C₂₄H₃₂N₃O₂	7.6	293.1648	237.1386	208.0756
17	1-Depropionyl- <i>N</i> -deethyl 1P-ETH-LAD	310.1913	C ₁₉ H ₂₄ N ₃ O	3.6	237.1386	208.0995	281.1522
3	1-Depropionyl- <i>N</i> ⁶ -deethyl 1P-ETH-LAD	310.1913	C ₁₉ H ₂₄ N ₃ O	5.3	209.1073	74.0964	237.1022
16	1-Depropionyl 1P-ETH-LAD	338.2226	C ₂₁ H ₂₈ N ₃ O	5.6	237.1386	208.0995	309.1835
18	1-Depropionyl-hydroxy 1P-ETH-LAD	354.2176	C ₂₁ H ₂₈ N ₃ O ₂	3.8	253.1335	297.1603	196.0762
22	<i>N</i> -Deethyl 1P-ETH-LAD	366.2176	C ₂₂ H ₂₈ N ₃ O ₂	5.9	293.1648	208.0995	237.1648
19	1-Depropionyl-dihydroxy 1P-ETH-LAD	370.2125	C ₂₁ H ₂₈ N ₃ O ₃	2.8	251.1178	279.1128	313.1552
20	1-Depropionyl-hydroxy 1P-ETH-LAD glucuronide	530.2496	C ₂₇ H ₃₆ N ₃ O ₈	2.4	253.1335	354.2176	325.1784

Table 1 (continued)

ID	Compound	Exact mass, m/z	Elemental composition	RT, min	FI A	FI B	FI C
23	AL-LAD	350.2226	C₂₂H₂₈N₃O	6.2	208.0995	309.1835	182.0838
24	<i>N</i> ⁶ -Deallyl- <i>N</i> -deethyl AL-LAD	282.1600	C ₁₇ H ₂₀ N ₃ O	3.2	209.1073	237.1027	134.0964
25	<i>N</i> ⁶ -Allyl-norlysergic acid	295.1441	C ₁₈ H ₁₉ N ₂ O ₂	2.9	70.0656	254.1049	238.0868
3	<i>N</i> ⁶ -Deallyl AL-LAD	310.1913	C ₁₉ H ₂₄ N ₃ O	5.3	209.1073	74.0964	237.1022
26	<i>N</i> -Deethyl AL-LAD	322.1913	C ₂₀ H ₂₄ N ₃ O	4.2	281.1522	208.0995	182.0838
27	<i>N</i> -Deethyl-hydroxy AL-LAD	338.1863	C ₂₀ H ₂₄ N ₃ O ₂	2.6	297.1471	225.1022	207.0916
28	Hydroxy AL-LAD isomer 1	366.2176	C ₂₂ H ₂₈ N ₃ O ₂	3.8	224.0944	325.1784	198.0787
29	Hydroxy AL-LAD isomer 2	366.2176	C ₂₂ H ₂₈ N ₃ O ₂	4.3	223.0871	325.1784	297.1603
30	Hydroxy AL-LAD isomer 3	366.2176	C ₂₂ H ₂₈ N ₃ O ₂	5.0	207.0922	247.1235	265.1340
31	Dihydroxy AL-LAD isomer 1	382.2125	C ₂₂ H ₂₈ N ₃ O ₃	3.3	221.0714	263.1178	313.1552
32	Dihydroxy AL-LAD isomer 2	382.2125	C ₂₂ H ₂₈ N ₃ O ₃	4.1	128.1069	255.1133	223.0871
33	Hydroxy AL-LAD isomer 1 glucuronide	542.2496	C ₂₈ H ₃₆ N ₃ O ₈	3.1	325.1784	224.0944	501.2105
34	ECPLA	336.2070	C₂₁H₂₆N₃O	6.0	223.1235	208.0756	86.0964
35	Lysergic acid amide	268.1444	C ₁₆ H ₁₈ N ₃ O	1.5	223.1235	208.0762	180.0813
36	Lysergic acid	269.1284	C ₁₆ H ₁₇ N ₂ O ₂	2.2	223.1235	254.1049	238.0868
37	<i>N</i> -Deethyl ECPLA	308.1757	C ₁₉ H ₂₂ N ₃ O	3.3	223.1235	208.0762	265.1340
38	<i>N</i> ⁶ -Demethyl ECPLA	322.1913	C ₂₀ H ₂₄ N ₃ O	5.9	209.1078	237.1027	86.0964
39	Hydroxy ECPLA isomer 1	352.2019	C ₂₁ H ₂₆ N ₃ O ₂	3.0	239.1184	224.0944	86.0964
40	Hydroxy ECPLA isomer 2	352.2019	C ₂₁ H ₂₆ N ₃ O ₂	4.0	239.1184	221.1078	334.1913
41	Hydroxy ECPLA isomer 3	352.2019	C ₂₁ H ₂₆ N ₃ O ₂	4.2	239.1184	86.0964	224.0706
42	Dihydroxy ECPLA	368.1968	C ₂₁ H ₂₆ N ₃ O ₃	3.3	237.1027	222.0555	86.0964
43	LSZ	336.2070	C₂₁H₂₆N₃O	5.3	223.1235	140.1070	208.0995
35	Lysergic acid amide	268.1444	C ₁₆ H ₁₈ N ₃ O	1.5	223.1235	208.0762	180.0813
36	Lysergic acid	269.1284	C ₁₆ H ₁₇ N ₂ O ₂	2.2	223.1235	254.1049	238.0868
44	Hydroxy lysergic acid amide	284.1393	C ₁₆ H ₁₈ N ₃ O ₂	1.0	221.1078	266.1287	239.1184
45	<i>N</i> ⁶ -Demethyl LSZ	322.1913	C ₂₀ H ₂₄ N ₃ O	5.2	209.1073	140.1070	237.1027
46	Hydroxy LSZ isomer 1	352.2019	C ₂₁ H ₂₆ N ₃ O ₂	3.7	239.1184	224.0711	140.1070
47	Hydroxy LSZ isomer 2	352.2019	C ₂₁ H ₂₆ N ₃ O ₂	3.9	221.1078	334.1913	249.1027
48	Hydroxy LSZ isomer 3	352.2019	C ₂₁ H ₂₆ N ₃ O ₂	4.3	208.0762	223.1235	334.1913
49	Dihydroxy LSZ	368.1968	C ₂₁ H ₂₆ N ₃ O ₃	2.8	237.1027	222.0555	265.0977
50	Hydroxy LSZ isomer 1 glucuronide	528.2340	C ₂₇ H ₃₄ N ₃ O ₈	2.1	239.1184	352.2019	140.1070
51	LSM-775	338.1863	C₂₀H₂₄N₃O₂	3.5	223.1235	208.0762	295.1446
52	<i>N</i> ⁶ -Demethyl LSM-775	324.1706	C ₁₉ H ₂₂ N ₃ O ₂	3.4	209.1078	237.1027	183.0922
53	Hydroxy LSM-775 isomer 1	354.1812	C ₂₀ H ₂₄ N ₃ O ₃	1.5	221.1078	336.1706	249.1027
54	Hydroxy LSM-775 isomer 2	354.1812	C ₂₀ H ₂₄ N ₃ O ₃	1.7	221.1078	336.1706	249.1027
55	Hydroxy LSM-775 isomer 3	354.1812	C ₂₀ H ₂₄ N ₃ O ₃	2.1	239.1184	224.0706	311.1395

(C₁₆H₁₇N₂O⁺) in comparison to m/z 281.1648 in the MS² spectrum of LSD. Other FI, for example, at m/z 223.1229 or m/z 208.0756, remained unchanged, whereas the FI at m/z 74.0964 was not detectable in the MS² spectrum of 1-depropionyl-*N*-deethyl 1P-LSD (ID 2). *N*⁶-Demethylation instead of *N*-deethylation resulted in formation of 1-depropionyl-*N*⁶-demethyl 1P-LSD (ID 3, PM at m/z 310.1913). The FI at m/z 223.1229 was shifted to m/z 209.1073 (C₁₄H₁₃N₂⁺) corresponding to the loss of methylene (− 14.0156 u, CH₂). Other FI, for example, at m/z 281.1648 or m/z 74.0964, were unchanged compared to LSD. Two isomers

of 1-depropionyl-hydroxy 1P-LSD (ID 4 and 5, PM at m/z 340.2019) were detectable. In the MS² spectrum of isomer 1 (ID 4, RT 3.4 min, Fig. 2), an initial loss of water (− 18.0105 u, H₂O) was detectable. Therefore, 1-depropionyl-hydroxy 1P-LSD isomer 1 was expected to carry an aliphatic hydroxy group. Based on the fragmentation pattern, a hydroxylation at the diethylamide part can be excluded because the FI at m/z 74.0964 was present in the MS² spectrum. Due to the detection of m/z 297.1597 (C₁₈H₂₁N₂O₂⁺), a hydroxylation at the *N*⁶-methyl group and position 7 can be excluded, which led to the indication that the hydroxy group might have been

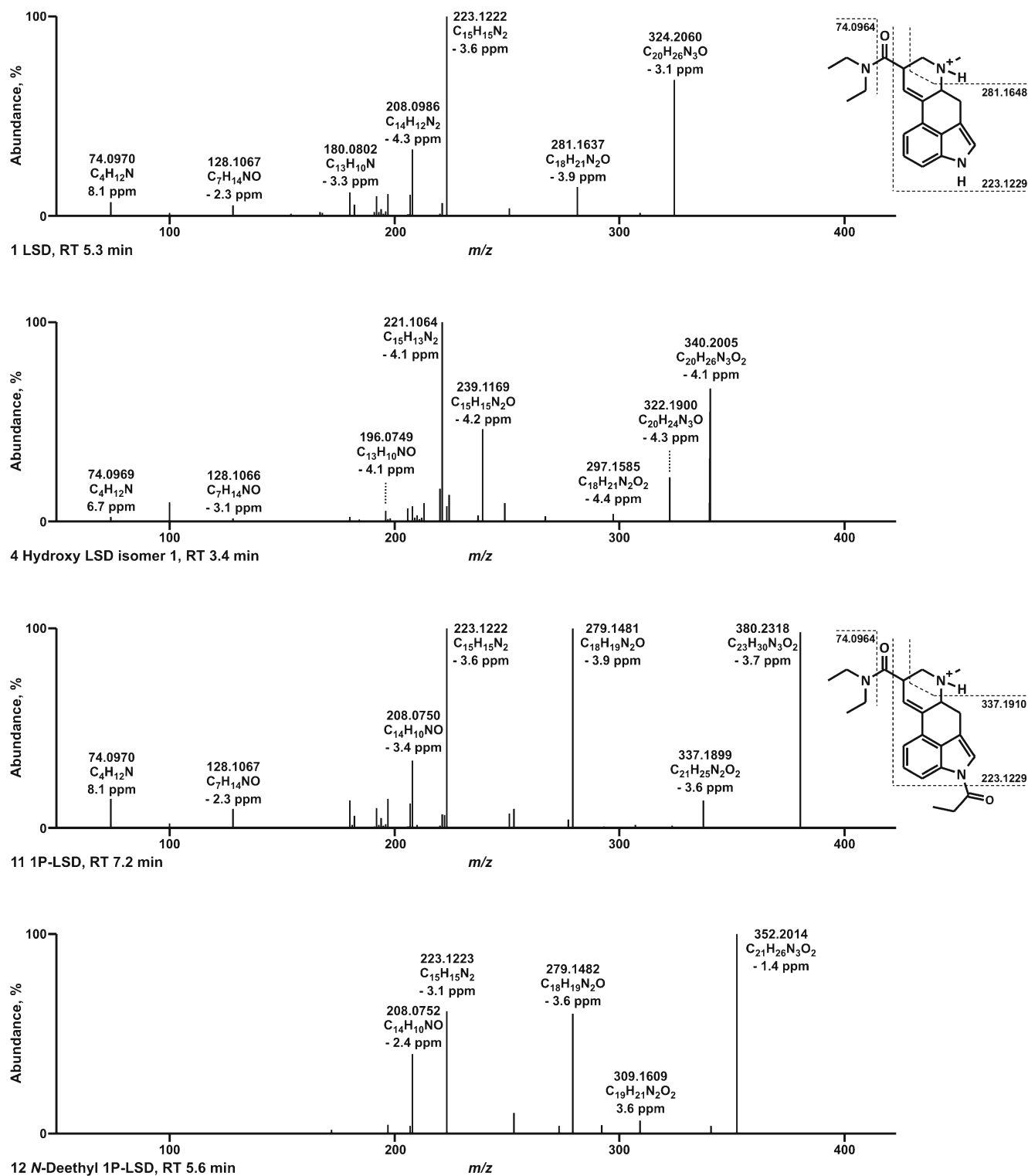


Fig. 2 HRMS/MS spectra and retention times (RT) of LSD (ID 1) and 1P-LSD (ID 11) as well as two of their metabolites (hydroxy LSD isomer 1, ID 4, and *N*-deethyl 1P-LSD, ID 12) to support described mass spectral-based metabolite identification. Numbering according to Table 1

located at position 4 or 5. However, an unambiguous assignment was not possible based on the fragmentation pattern in the MS² spectrum. In the case of 1-depropionyl-hydroxy 1P-LSD isomer 2 (ID 5, RT 3.6 min), no water loss was detectable

and the hydroxy group should therefore most likely be located at an aromatic position [48]. The FI at *m/z* 74.0964 and *m/z* 297.1597 were both present. Due to these FI, the hydroxy group is most probably located at the indole part of the 9,10-

didehydroergoline core. Furthermore, 1-depropionyl-dihydroxy 1P-LSD (ID 6, PM at m/z 356.1968) was detected with one aliphatic and one aromatic hydroxy group. Due to the fragmentation pattern, this metabolite could be the result of the combination of both monohydroxy isomers (ID 4 and 5). However, the metabolite 2-oxo-3-hydroxy LSD was reported to be the main urinary excretion product of LSD [19, 41]. Possible metabolic pathways resulting in its formation were discussed by Klette et al. [40]. Nevertheless, its protonated mass at m/z 356 corresponds to the mass of 1-depropionyl-dihydroxy 1P-LSD (ID 6). Also, the prominent FI at m/z 237 and m/z 338 described by Klette et al. were present in the spectrum of 1-depropionyl-dihydroxy 1P-LSD (ID 6). Due to this fact and the proposed fragmentation pattern, both compounds were expected to be identical. The aforementioned metabolites of 1P-LSD were also found in incubations with LSD and are therefore not suitable as urinary markers to discriminate between the intake of LSD and 1P-LSD. In general, structurally identical metabolites have the same ID in Table 1 to highlight these observations. Nevertheless, two 1P-LSD metabolites not evolved from LSD were identified. These metabolites were formed from 1P-LSD by *N*-deethylation (ID 12, PM at m/z 352.2019) and *N*⁶-demethylation (ID 13, PM at m/z 366.2176), respectively. In the case of *N*-deethyl 1P-LSD (ID 12, Fig. 2), the FI at m/z 309.1597 ($C_{19}H_{21}N_2O_2^+$) corresponded to the FI at m/z 337.1910 in the spectrum of 1P-LSD shifted by -28.0313 u, the loss of an ethylene group (C_2H_4). The FI at m/z 279.1491 was unchanged. In the case of *N*⁶-demethyl 1P-LSD (1P-nor-LSD) (ID 13), the FI at m/z 279.1491 was shifted by -14.0156 u due to the loss of methylene (CH_2), while the FI at m/z 337.1910 was unchanged. However, it is possible that *N*⁶-demethyl 1P-LSD (ID 13) was also generated during the metabolic transformation of 1P-ETH-LAD, although it was not detected in the pS9 incubations. In conclusion, *N*-deethyl 1P-LSD (ID 12) was the only metabolite that could only be formed from 1P-LSD and from no other LSD-type NPS investigated in this study. LSD could also be formed after intake of ALD-52 or 1B-LSD, and in both cases, LSD and its metabolites were detected in the pS9 incubations. In the case of ALD-52, the two specific metabolites *N*-deethyl ALD-52 (ID 9, PM at m/z 338.1863) and *N*⁶-demethyl ALD-52 (nor-ALD-52) (ID 10, PM at m/z 352.2019) were additionally identified, and in the case of 1B-LSD, only hydroxy 1B-LSD (ID 15, PM at m/z 410.2438) was detected. These findings clearly demonstrated that urinary screening results have to be interpreted with care and that a positive urine screening result for LSD or its metabolites must not always be caused by an intake of LSD itself.

Proposed metabolic pathways

The proposed metabolic pathways of 1P-LSD are given in Fig. 3. The proposed metabolic pathways and MS² data of

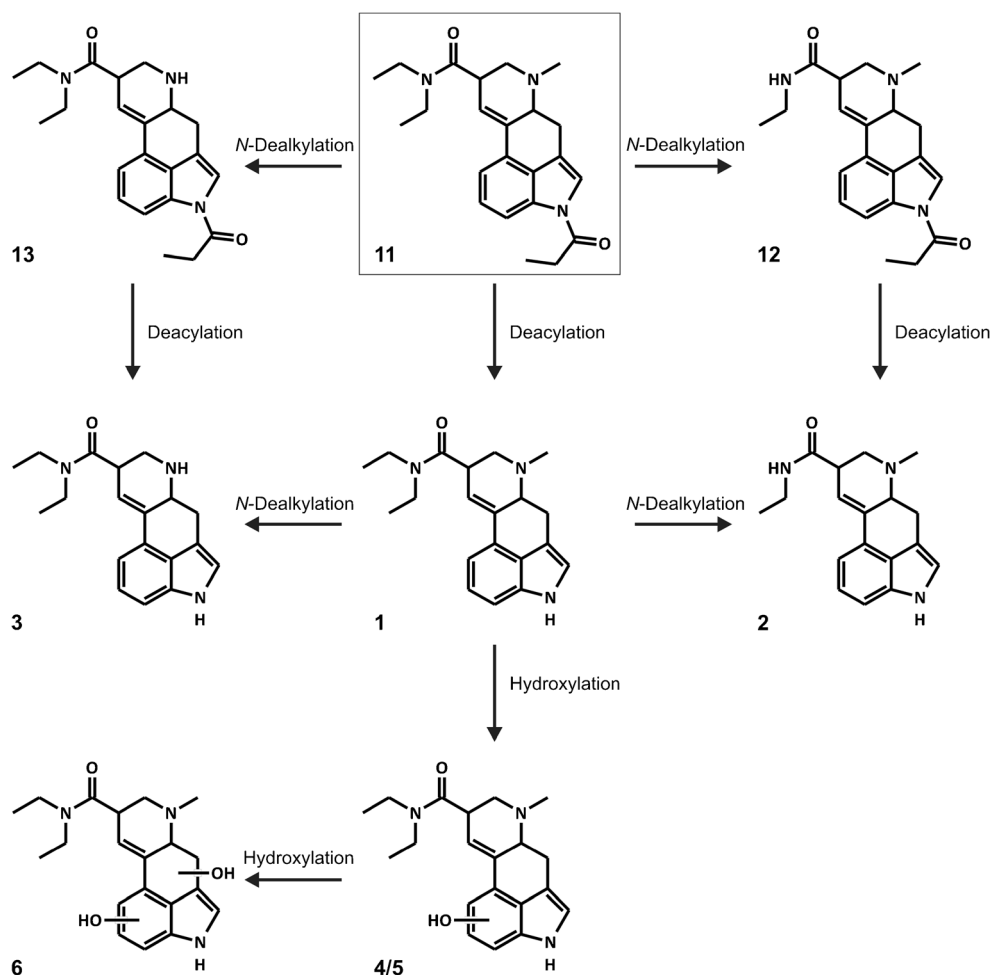
the other compounds can be found in the ESM (Figs. S1–S10).

Monooxygenases activity screening and inhibition studies using selective CYP inhibitors

In order to investigate the ability of monooxygenases to catalyze the initial metabolic phase I steps, an activity screening study using the ten most important CYP isoenzymes and FMO3 was performed. Incubations with pHLM were used as control. These data are only qualitative and do not reflect a quantitative contribution of the investigated monooxygenases to hepatic clearance. Such an assessment requires the collection of enzyme kinetic data or inhibition experiments [31, 32, 49]. Results are listed in Table 2. CYP3A4 was not only found to be involved in the *N*⁶-deallylation of LSD, ALD-52, 1P-LSD, 1B-LSD, ECPLA, LSZ, and LSM-775, but also in the *N*⁶-deethylation of ETH-LAD and 1P-ETH-LAD and *N*⁶-dealkylation of AL-LAD. Only in the case of LSD did CYP2C19 show additional *N*⁶-demethylation activity. CYP3A4 also catalyzed the *N*-deethylation of LSD and all other lysergamide test drugs, which resulted in the formation of *N*-mono ethylamide analog. Only CYP2C9 also catalyzed the *N*-deethylation of LSD and ECPLA. Aliphatic or aromatic hydroxylations were also catalyzed by CYP3A4 for all investigated test drugs and additionally by CYP1A2 with the exception of the 1-acylated LSD derivatives and ETH-LAD. CYP2D6 was found to be involved in the hydroxylation of ALD-52, 1B-LSD, and ETH-LAD. In pHLM incubations, the 1-deacylation of ALD-52, 1P-LSD, 1B-LSD, and 1P-ETH-LAD was additionally observed. However, this step was expected to be catalyzed by amidases and was not observed in incubations with the recombinant monooxygenases. In pHLM incubations with AL-LAD, ECPLA, and LSZ, also the corresponding lysergic acid metabolite was detected, and in the case of ECPLA and LSZ, also lysergic acid amide. However, these metabolites could not be detected in incubations with recombinant enzymes and may also be the result of amidase-catalyzed reactions.

The involvement of CYP1A2 and especially CYP3A4 in the metabolism of the investigated lysergamides is noteworthy. To confirm these results and to assess the importance of their contribution to the metabolism of these substances in the human liver, pHLM incubations in the presence of selective CYP inhibitors were performed [32]. LSD, 1B-LSD, ETH-LAD, AL-LAD, ECPLA, LSZ, and LSM-775 were incubated with the CYP1A2 inhibitor alpha-naphthoflavone and the CYP3A4 inhibitor ketoconazole or a mixture of them. For ALD-52, 1P-LSD, 1B-LSD, ETH-LAD, and 1P-ETH-LAD, only ketoconazole was used because only CYP3A4 was shown to be involved in their initial metabolic steps. Results are summarized in Fig. 4. Formation of CYP-dependent metabolites in reference incubations without inhibitor was set to 100% and compared to metabolite formation in incubations with inhibitor. For all test drugs, a significant reduction of metabolite formation in incubations with

Fig. 3 Postulated metabolic pathways of 1P-LSD studied by in vitro incubations with pooled human liver S9 fraction. Numbering according to Table 1



inhibitors was observed. In the case of LSD, co-incubations with alpha-naphthoflavone decreased the metabolite formation by more than 50% and with ketoconazole and a mixture of both inhibitors by more than 80% in comparison to the incubations without an inhibitor. Metabolite formation in co-incubations of the 1-acylated lysergamides (ALD-52, 1P-LSD, 1B-LSD, and 1P-ETH-LAD) with ketoconazole was reduced by more than 80%. In the case of ETH-LAD, ketoconazole led to a reduction of the metabolite formation by around 70%. The formation of AL-LAD, ECPLA, and LSZ metabolites was significantly increased by both inhibitors, alpha-naphthoflavone and ketoconazole, and co-incubations with their mixture resulted in a decrease of more than 70% in the case of AL-LAD and around 90% for ECPLA and LSZ. Only in the case of LSM-775 did co-incubations with alpha-naphthoflavone not result in a statistically significant reduction of formed metabolites, in contrast to co-incubations with ketoconazole and their mixture that led to decreased metabolite formation of around 70% or 80%, respectively. Residual metabolite formations were most probably caused by incomplete enzyme inhibition and/or the involvement of further CYP isoforms in the metabolic transformation of the test drugs. Nevertheless, the inhibition experiments confirmed the

importance of CYP1A2 and especially CYP3A4 in the metabolism of LSD analogs. CYP1A2 is known to be expressed polymorphically in humans, resulting in large interindividual variation of activity [50]. For example, polymorphisms resulting in lower CYP1A2 activity may lead to a decreased metabolic transformation of LSD-like substances that could result in an increased half-life of the drug. However, the results of the inhibition experiments suggest that CYP3A4 is even more important in the metabolism of LSD-related substances. Inhibition of CYP3A4 by co-consumed drugs or food ingredients may also lead to decreased metabolic transformation. Nevertheless, LSD is not expected to exhibit remarkable acute toxicity [51, 52], but nothing is known about the toxicity of the LSD-based NPS.

Toxicological detectability

For toxicological detectability studies, a dose of 0.01 mg/kg BW was administered to rats. Assuming a human BW of 60 kg, the doses corresponded to an expected recreational dose of 136 µg in accordance with the dose by factor approach [53]. The SUSAs by GC-MS, LC-MSⁿ, and LC-HRMS/MS were used and the results are briefly described in the following.

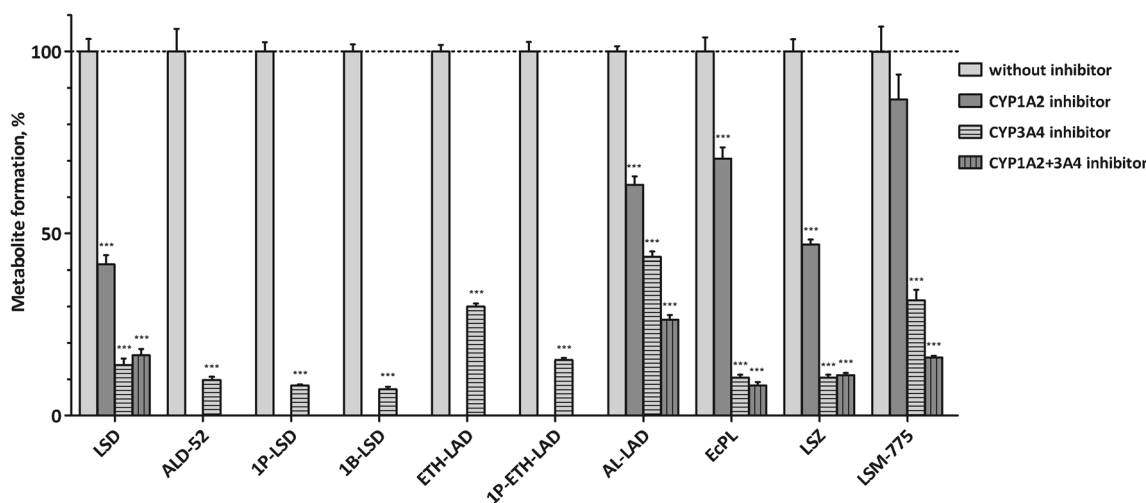


Fig. 4 Percentage formation of CYP-dependent metabolites in pHLM co-incubations of LSD or LSD analogs with the selective CYP1A2 inhibitor alpha-naphthoflavone, the selective CYP3A4 inhibitor ketoconazole, or a

mixture of both inhibitors. Formation in reference incubations without inhibitor was referred to as 100%

GC-MS standard urine screening approach

No metabolites or parent compounds could be identified in the rat urine by the GC-MS SUSA. This was most probably caused by the low stability of LSD and its derivatives against acidic hydrolysis and heat [54]. Nevertheless, the sample preparation was not changed as this is an established procedure used in toxicological routine analysis [39, 55]. Another reason could be minor excretion in rat urine and/or insufficient sensitivity of the used GC-MS apparatus. Also at and below

100 ng/mL of methanolic pure substance solutions, the GC-MS procedure was not able to detect the analytes.

LC-MSⁿ standard urine screening approach

No metabolites or parent compounds could be identified in the rat urine by the LC-MSⁿ SUSA, most probably caused by insufficient sensitivity. The LOIs using methanolic pure substance solutions were as follows: 1 ng/mL for 1P-LSD; 10 ng/mL for LSD, ALD-52, ETH-LAD, AL-LAD, ECPLA, LSZ, and LSM-775; and 100 ng/mL for 1B-LSD and 1P-ETH-LAD. One reason for the lack of sensitivity might be the extremely broad peaks under the used standard conditions.

Table 2 General involvement of tested monooxygenases in the initial metabolic steps. *n.d.*, not detected

Compound	N ⁶ -Dealkylation	N-Deethylation	Hydroxylation
LSD	CYP2C19	CYP2C9	CYP1A2
	CYP3A4	CYP3A4	CYP3A4
ALD-52	CYP3A4	CYP3A4	CYP2D6
			CYP3A4
1P-LSD	CYP3A4	CYP3A4	CYP3A4
1B-LSD	CYP3A4	CYP3A4	CYP2D6
			CYP3A4
ETH-LAD	CYP3A4	CYP3A4	CYP2D6
			CYP3A4
1P-ETH-LAD	CYP3A4	CYP3A4	CYP3A4
AL-LAD	CYP3A4	CYP3A4	CYP1A2
			CYP3A4
ECPLA	CYP2C19	CYP2C9	CYP1A2
	CYP3A4	CYP3A4	CYP3A4
LSZ	CYP3A4	n.d.	CYP1A2
			CYP3A4
LSM-775	CYP3A4	n.d.	CYP1A2
			CYP3A4

LC-HRMS/MS standard urine screening approach

Only a single ALD-52 metabolite, 1-deacetyl-N-deethyl ALD-52 (ID 2), was identified in the rat urine samples after a recreational user's dose. However, this metabolite is not unique and can also be formed after intake of LSD, 1P-LSD, or 1B-LSD. No other metabolites or parent compounds could be identified by the LC-HRMS/MS SUSA. The LOIs using methanolic pure substance solutions were as follows: 1 ng/mL for LSD, 1P-LSD, ETH-LAD, AL-LAD, ECPLA, and LSZ; and 10 ng/mL for ALD-52, 1B-LSD, 1P-ETH-LAD, and LSM-775.

Therefore, for detection and differentiation of an intake of LSD or its derivatives after expected recreational doses, a more selective sample workup, concentration step, and more selective MS settings may help in detecting the parent drugs and/or unique metabolites identified in this study. For example, solid-phase extraction by mixed-mode cartridges, optionally after enzymatic conjugate cleavage, followed by LC-HRMS/MS using an adapted separation method and selective product ion scan or multiple-reaction monitoring should meet these requests.

Conclusions

The present study demonstrated that ALD-52, 1P-LSD, 1B-LSD, ETH-LAD, 1P-ETH-LAD, AL-LAD, ECPLA, LSZ, and LSM-775 were biotransformed to several phase I and few phase II metabolites in vitro. Many metabolites can originate from different parent compounds making their differentiation difficult, but this study also identified unique metabolites overcoming this problem. The mass spectral data obtained during these studies is essential for establishing reliable detection methods, especially for urinalysis. However, selective sample workup and MS settings are needed for reliable analytical detection and differentiation. CYP1A2, CYP2C9, CYP2C19, CYP2D6, and CYP3A4 were found to be involved in the initial metabolic steps. Inhibition experiments confirmed the major influence of CYP1A2 and CYP3A4; therefore, genetic polymorphisms of CYP1A2 might have an impact on the metabolism of these NPS. Furthermore, drug–drug or drug–food interactions might occur in case of co-consumption with CYP1A2 or CYP3A4 inhibitors resulting in decreased metabolic transformation of LSD analogs, but further investigations are needed for an assessment of possible clinical effects. The authors' standard urine screening procedures are most likely not able to allow the detection of the studied NPS. Alternative analytical strategies need to be used instead.

Acknowledgments The authors would like to thank Amin A. Weber and the *Stiftelsen för Klinisk farmakologi & farmakoterapi* for support.

Compliance with ethical standards

The studies have been approved by an ethics committee (Landesamt für Verbraucherschutz, Saarbrücken, Germany).

Conflict of interest The authors declare that they have no conflict of interest.

Publisher's Note Springer Nature remains neutral with regard to jurisdictional claims in published maps and institutional affiliations.

References

- Stevens J. *Storming heaven: LSD and the American dream*. New York: Grove Press; 1987.
- Hoffman AJ, Nichols DE. Synthesis and LSD-like discriminative stimulus properties in a series of N(6)-alkyl norlysergic acid N,N-diethylamide derivatives. *J Med Chem*. 1985;28(9):1252–5.
- Oberlender R, Pfaff RC, Johnson MP, Huang XM, Nichols DE. Stereoselective LSD-like activity in d-lysergic acid amides of (R)- and (S)-2-aminobutane. *J Med Chem*. 1992;35(2):203–11.
- Huang X, Marona-Lewicka D, Pfaff RC, Nichols DE. Drug discrimination and receptor binding studies of N-isopropyl lysergamide derivatives. *Pharmacol Biochem Behav*. 1994;47(3):667–73.
- Monte AP, Marona-Lewicka D, Kanthasamy A, Sanders-Bush E, Nichols DE. Stereoselective LSD-like activity in a series of d-lysergic acid amides of (R)- and (S)-2-aminoalkanes. *J Med Chem*. 1995;38(6):958–66.
- Nichols DE, Frescas S, Marona-Lewicka D, Kurrasch-Orbaugh DM. Lysergamides of isomeric 2,4-dimethylazetidines map the binding orientation of the diethylamide moiety in the potent hallucinogenic agent N,N-diethyllysergamide (LSD). *J Med Chem*. 2002;45(19):4344–9.
- Shulgin A, Shulgin A. *Tihkal: the continuation*. Berkeley: Transform Press; 1997.
- Pfaff RC, Huang X, Marona-Lewicka D, Oberlender R, Nichols DE. Lysergamides revisited. *NIDA Res Monogr*. 1994;146:52–73.
- Nichols DE. LSD and its lysergamide cousins. *Heffter Rev Psychedelic Res*. 2001;2:80–7.
- Nichols DE. *Psychedelics*. *Pharmacol Rev*. 2016;68(2):264–355.
- Nichols DE. Dark classics in chemical neuroscience: lysergic acid diethylamide (LSD). *ACS Chem Neurosci*. 2018;9(10):2331–43.
- Liechti ME. *Modern clinical research on LSD*. *Neuropsychopharmacology*. 2017;42(11):2114–27.
- Brandt SD, Kavanagh PV, Westphal F, Stratford A, Elliott SP, Hoang K, et al. Return of the lysergamides. Part I: analytical and behavioural characterization of 1-propionyl-d-lysergic acid diethylamide (1P-LSD). *Drug Test Anal*. 2016;8(9):891–902.
- Brandt SD, Kavanagh PV, Westphal F, Elliott SP, Wallach J, Stratford A, et al. Return of the lysergamides. Part III: analytical characterization of N(6)-ethyl-6-norlysergic acid diethylamide (ETH-LAD) and 1-propionyl ETH-LAD (1P-ETH-LAD). *Drug Test Anal*. 2017;9(10):1641–9.
- Brandt SD, Kavanagh PV, Westphal F, Elliott SP, Wallach J, Colestock T, et al. Return of the lysergamides. Part II: analytical and behavioural characterization of N(6)-allyl-6-norlysergic acid diethylamide (AL-LAD) and (2'S,4'S)-lysergic acid 2,4-dimethylazetidide (LSZ). *Drug Test Anal*. 2017;9(1):38–50.
- Halberstadt AL, Klein LM, Chatha M, Valenzuela LB, Stratford A, Wallach J, et al. Pharmacological characterization of the LSD analog N-ethyl-N-cyclopropyl lysergamide (ECPLA). *Psychopharmacology*. 2018. <https://doi.org/10.1007/s00213-018-5055-9>.
- Brandt SD, Kavanagh PV, Twamley B, Westphal F, Elliott SP, Wallach J et al. Return of the lysergamides. Part IV: Analytical and pharmacological characterization of lysergic acid morpholide (LSM-775). *Drug Test Anal*. 2018;10(2):310–22.
- EMCDDA. *European drug report 2017: trends and developments*. Publications of the European Union 2017.
- Canez J, Cailleux A, Turcant A, Le Bouil A, Harry P, Allain P. Determination of LSD and its metabolites in human biological fluids by high-performance liquid chromatography with electrospray tandem mass spectrometry. *J Chromatogr B Biomed Sci Appl*. 2001;765(1):15–27.
- Dolder PC, Liechti ME, Rentsch KM. Development and validation of a rapid turboflow LC-MS/MS method for the quantification of LSD and 2-oxo-3-hydroxy LSD in serum and urine samples of emergency toxicological cases. *Anal Bioanal Chem*. 2015;407(6):1577–84.
- Dolder PC, Schmid Y, Haschke M, Rentsch KM, Liechti ME. Pharmacokinetics and Concentration-Effect Relationship of Oral LSD in Humans. *Int J Neuropsychopharmacol*. 2015;19(1).
- Diao X, Huestis MA. Approaches, challenges, and advances in metabolism of new synthetic cannabinoids and identification of optimal urinary marker metabolites. *Clin Pharmacol Ther*. 2017;101(2):239–53.
- Welter-Luedeke J, Maurer HH. New psychoactive substances: chemistry, pharmacology, metabolism, and detectability of amphetamine derivatives with modified ring systems. *Ther Drug Monit*. 2016;38(1):4–11.
- Meyer MR. New psychoactive substances: an overview on recent publications on their toxicodynamics and toxicokinetics. *Arch Toxicol*. 2016;90(10):2421–44.

25. Meyer MR. Toxicokinetics of NPS: update 2017. *Handb Exp Pharmacol*. 2018. https://doi.org/10.1007/164_2018_102.
26. Mogler L, Wilde M, Huppertz LM, Weinfurter G, Franz F, Auwärter V. Phase I metabolism of the recently emerged synthetic cannabinoid CUMYL-PEGACLONE and detection in human urine samples. *Drug Test Anal*. 2018;10(5):886–91.
27. Watanabe S, Vikingsson S, Roman M, Green H, Kronstrand R, Wohlfarth A. In vitro and in vivo metabolite identification studies for the new synthetic opioids acetylfentanyl, acrylfentanyl, furanylfentanyl, and 4-fluoro-isobutyrylfentanyl. *AAPS J*. 2017;19(4):1102–22.
28. Welter J, Meyer MR, Wolf EU, Weinmann W, Kavanagh P, Maurer HH. 2-Methiopropamine, a thiophene analogue of methamphetamine: studies on its metabolism and detectability in the rat and human using GC-MS and LC-(HR)-MS techniques. *Anal Bioanal Chem*. 2013;405(10):3125–35.
29. Richter LHJ, Flockerzi V, Maurer HH, Meyer MR. Pooled human liver preparations, HepaRG, or HepG2 cell lines for metabolism studies of new psychoactive substances? A study using MDMA, MDD, butylone, MDP, MDPV, MDPB, 5-MAPB, and 5-API as examples. *J Pharm Biomed Anal*. 2017;143:32–42.
30. Chauret N, Gauthier A, Nicoll-Griffith DA. Effect of common organic solvents on in vitro cytochrome P450-mediated metabolic activities in human liver microsomes. *Drug Metab Dispos*. 1998;26(1):1–4.
31. Wagmann L, Meyer MR, Maurer HH. What is the contribution of human FMO3 in the N-oxygenation of selected therapeutic drugs and drugs of abuse? *Toxicol Lett*. 2016;258:55–70.
32. Meyer GM, Meyer MR, Wink CS, Zapp J, Maurer HH. Studies on the in vivo contribution of human cytochrome P450s to the hepatic metabolism of glaucine, a new drug of abuse. *Biochem Pharmacol*. 2013;86(10):1497–506.
33. Wagmann L, Brandt SD, Kavanagh PV, Maurer HH, Meyer MR. In vitro monoamine oxidase inhibition potential of alpha-methyltryptamine analog new psychoactive substances for assessing possible toxic risks. *Toxicol Lett*. 2017;272:84–93.
34. Welter J, Kavanagh P, Meyer MR, Maurer HH. Benzofuran analogues of amphetamine and methamphetamine: studies on the metabolism and toxicological analysis of 5-APB and 5-MAPB in urine and plasma using GC-MS and LC-(HR)-MS(n) techniques. *Anal Bioanal Chem*. 2015;407(5):1371–88.
35. Helfer AG, Michely JA, Weber AA, Meyer MR, Maurer HH. Orbitrap technology for comprehensive metabolite-based liquid chromatographic-high resolution-tandem mass spectrometric urine drug screening—exemplified for cardiovascular drugs. *Anal Chim Acta*. 2015;891:221–33.
36. Caspar AT, Westphal F, Meyer MR, Maurer HH. LC-high resolution-MS/MS for identification of 69 metabolites of the new psychoactive substance 1-(4-ethylphenyl)-N-[(2-methoxyphenyl)methyl]propane-2-amine (4-EA-NBOMe) in rat urine and human liver S9 incubates and comparison of its screening power with further MS techniques. *Anal Bioanal Chem*. 2018;410(3):897–912.
37. Wissenbach DK, Meyer MR, Remane D, Philipp AA, Weber AA, Maurer HH. Drugs of abuse screening in urine as part of a metabolite-based LC-MSn screening concept. *Anal Bioanal Chem*. 2011;400(10):3481–9.
38. Meyer MR, Lindauer C, Welter J, Maurer HH. Dimethocaine, a synthetic cocaine analogue: studies on its in-vivo metabolism and its detectability in urine by means of a rat model and liquid chromatography-linear ion-trap (high-resolution) mass spectrometry. *Anal Bioanal Chem*. 2014;406(7):1845–54.
39. Maurer HH, Pflieger K, Weber AA. Mass spectral data of drugs, poisons, pesticides, pollutants and their metabolites. Wiley-VCH: Weinheim; 2016.
40. Klette KL, Anderson CJ, Poch GK, Nimrod AC, ElSohly MA. Metabolism of lysergic acid diethylamide (LSD) to 2-oxo-3-hydroxy LSD (O-H-LSD) in human liver microsomes and cryopreserved human hepatocytes. *J Anal Toxicol*. 2000;24(7):550–6.
41. Poch GK, Klette KL, Hallare DA, Manglicmot MG, Czarny RJ, McWhorter LK, et al. Detection of metabolites of lysergic acid diethylamide (LSD) in human urine specimens: 2-oxo-3-hydroxy-LSD, a prevalent metabolite of LSD. *J Chromatogr B Biomed Sci Appl*. 1999;724(1):23–33.
42. Steuer AE, Poetzsch M, Stock L, Eisenbeiss L, Schmid Y, Liechti ME, et al. Development and validation of an ultra-fast and sensitive microflow liquid chromatography-tandem mass spectrometry (MFLC-MS/MS) method for quantification of LSD and its metabolites in plasma and application to a controlled LSD administration study in humans. *Drug Test Anal*. 2017;9(5):788–97.
43. Dolder PC, Liechti ME, Rentsch KM. Development and validation of an LC-MS/MS method to quantify lysergic acid diethylamide (LSD), iso-LSD, 2-oxo-3-hydroxy-LSD, and nor-LSD and identify novel metabolites in plasma samples in a controlled clinical trial. *J Clin Lab Anal*. 2018;32(2).
44. Favretto D, Frison G, Maietti S, Ferrara SD. LC-ESI-MS/MS on an ion trap for the determination of LSD, iso-LSD, nor-LSD and 2-oxo-3-hydroxy-LSD in blood, urine and vitreous humor. *Int J Legal Med*. 2007;121(4):259–65.
45. Jang M, Kim J, Han I, Yang W. Simultaneous determination of LSD and 2-oxo-3-hydroxy LSD in hair and urine by LC-MS/MS and its application to forensic cases. *J Pharm Biomed Anal*. 2015;115:138–43.
46. Johansen SS, Jensen JL. Liquid chromatography-tandem mass spectrometry determination of LSD, ISO-LSD, and the main metabolite 2-oxo-3-hydroxy-LSD in forensic samples and application in a forensic case. *J Chromatogr B Anal Technol Biomed Life Sci*. 2005;825(1):21–8.
47. Richter LHJ, Maurer HH, Meyer MR. New psychoactive substances: studies on the metabolism of XLR-11, AB-PINACA, FUB-PB-22, 4-methoxy-alpha-PVP, 25-I-NBOMe, and meclonazepam using human liver preparations in comparison to primary human hepatocytes, and human urine. *Toxicol Lett*. 2017;280:142–50.
48. Niessen WM, Correa RA. Interpretation of MS-MS mass spectra of drugs and pesticides. Hoboken: Wiley; 2016.
49. Wink CS, Meyer GM, Meyer MR, Maurer HH. Toxicokinetics of lefetamine and derived diphenylethylamine designer drugs—contribution of human cytochrome P450 isozymes to their main phase I metabolic steps. *Toxicol Lett*. 2015;238(3):39–44.
50. Koonrungsesomboon N, Khatsri R, Wongchompoo P, Teekachunhatean S. The impact of genetic polymorphisms on CYP1A2 activity in humans: a systematic review and meta-analysis. *Pharmacogenomics J*. 2018;18(6):760–8.
51. Nichols DE, Grob CS. Is LSD toxic? *Forensic Sci Int*. 2018;284:141–5.
52. Passie T, Halpern JH, Stichtenoth DO, Emrich HM, Hintzen A. The pharmacology of lysergic acid diethylamide: a review. *CNS Neurosci Ther*. 2008;14(4):295–314.
53. Sharma V, McNeill JH. To scale or not to scale: the principles of dose extrapolation. *Br J Pharmacol*. 2009;157(6):907–21.
54. Crews C. Analysis of ergot alkaloids. *Toxins (Basel)*. 2015;7(6):2024–50.
55. Meyer MR, Schmitt S, Maurer HH. Studies on the metabolism and detectability of the emerging drug of abuse diphenyl-2-pyrrolidinemethanol (D2PM) in rat urine using GC-MS and LC-HR-MS/MS. *J Mass Spectrom*. 2013;48(2):243–9.